Synthesis and Biological Activity of 3-(Heteroaryl)quinolin-2(1H)-ones Bis-Heterocycles as Potential Inhibitors of the Protein Folding Machinery Hsp90

Enrique Larghi, Alexandre Bruneau, Félix Sauvage, Mouad Alami, Juliette Vergnaud-Gauduchon, Samir Messaoudi

Communication

Synthesis and Biological Activity of 3-(heteroaryl)quinolin-2(1*H*)-ones bis-Hetereocycles as potential Inhibitors of the Protein Folding Machinery Hsp90

Enrique L. Larghi,[a,b,*] Alexandre Bruneau,[b] Félix Sauvage,[c] Mouad Alami,[b] Juliette Vergnaud-Gauduchon[c] and Samir Messaoudi [a,*]

[a] Université Paris-Saclay, CNRS, BioCIS, 92290, Châtenay-Malabry, France;
[b] Instituto de Química Rosario (IQUIR) CONICET/UNR, FBioyF, Rosario, S2002LRK, Argentina;
[c] Université Paris-Saclay, CNRS, Institut Galien-Paris Saclay, 92296 Châtenay-Malabry, France.
* Correspondence: larghi@iquir-conicet.gov.ar; samir.messaoudi@universite-paris-saclay.fr

Received:

Abstract: In the context of pursue our SAR study around 6BrCaQ analogues as C-terminal Hsp90 inhibitors, we designed and synthesized during this study a novel series of 3-(heteroaryl)quinolin-2(*1H*)-ones of type **3, 4** and **5** as a novel class of 6BrCaQ analogues. A Pd-catalyzed Liebeskind-Srogl cross-coupling was developed as a convenient approach for an easy access to complex purine architectures. This series of analogues showed a promising biological effect against MDA-MB231 and PC-3 cancer cell lines. This study led to the identification of the best compounds **3b** (IC_{50} = 28 μM) and **4e** which induce a significant decrease of CDK-1 client protein and stabilize the levels of Hsp90 and Hsp70 without triggering the HSR response.

Keywords: Hsp90, 6BrCaQ, 3-(heteroaryl)quinolin-2(*1H*)-ones, purines, cytotoxicity.

1. Introduction

The 90-kDa heat shock protein (Hsp90) has emerged recently as a promising therapeutic target for the treatment of cancer [1-5] and other diseases [6-7]. As a chaperone protein, Hsp90 is evolved in the conformational maturation, folding, stabilization, activation, and degradation of over 400 client proteins in healthy cells as well as in cancerous cells which are directly associated with all hallmarks of cancer [8-11]. This Hsp90 chaperone cycle depends on the ATPase activity. ATP binding to the N-terminal domain (NTD) and hydrolysis by Hsp90 drive a conformational cycle necessary for chaperone function [12-14]. Binding of ATP to each monomer shifts Hsp90 to a "closed" formation that can bind, fold, and activate client proteins [15,16]. Thus, inhibition of Hsp90 function results in simultaneous interruption of many signal transduction pathways, which are pivotal to tumor progression and survival.

Several structurally distinct Hsp90 inhibitors that target the ATP binding pocket are currently being evaluated for anticancer activity in numerous Phase II and several Phase III clinical trials, however, they are ineffective over time due to the compensatory mechanism involving induction of a heat shock response. The expression of chaperones Hsp27, Hsp70, Hsp40, and Hsp90 increase [17-19] leading to undesirable chemoprotective effects [20-22]. Clinical resistance has been attributed to this chemoprotective effect, and dosage increases to overcome resistance are not a viable option due to toxicity. These results are motivating the pursuit of alternative strategies for modulating heat shock protein complexes [23-25].

An alternative molecular mechanism of inhibition is through binding to the C-terminal domain of Hsp90. The CTD has been implicated biochemically as the site of a possible second, cryptic ATP-binding site on the protein. Its contribution to the overall regulation of chaperone function is not clear, but some small molecules that interact with the C-terminal domain such as the antibiotic novobiocin [26] (Nvb, Figure 1) and coumermycin A1 (Cm A1), induce client protein degradation without heat shock response induction [27-31], giving new promise to Hsp90 inhibition for cancer treatments.

In this context, we previously reported a novel series of simplified **3** amido-quinolin-2-one analogues related to Nvb as a class of highly potent hsp90 inhibitors. [32-36] From the structure-relationship activity (SAR) studies, 6BrCaQ (Figure 1) [37, 38] was identified a very promising C-terminal Hsp90 inhibitor displaying an antiproliferative activity ranging LC_{50} of 5-50 µM [39, 40] against various cancer cell lines (MCF7, MDA MB231, Caco2, IGROV, ISHIKAWA, PC3 and HT29 cells). Further studies on its mode of action revealed that 6BrCaQ manifests downregulation of several Hsp90 client proteins (HER2, Raf-1 and cdk-4), induces a high apoptosis level in MCF-7 breast cancer cell line and PC3. In addition, encapsulated in liposomes, 6BrCaQ exerted an improved *in vitro* activity on breast cancer cells (MDA-MB-231) and displays an *in vivo* anti-tumor activity on an orthotopic breast cancer model in nude mice [40].

More recently, we demonstrated that conjugation of 6BrCaQ with the cationic head triphenylphosphonium (TPP) leads to the conjugate 6BrCaQ-C10-TPP for the targeting of the mitochondrial heat shock protein TRAP1. 6BrCaQ-C10-TPPdisplays an anti-proliferative activity with mean GI_{50} values at a nanomolar level in a diverse set of human cancer cells (GI_{50} = 0.008-0.30 µM) including MDA-MB-231, HT-29, HCT116, K562 and PC-3 cancer cell lines. This study showed that this compound 6BrCaQ-C_{10}-TPP induces a significant mitochondrial membrane disruption and interfere with TRAP1 function in colon carcinoma cells without inducing the heat-shock response HSF1 [41].

On the other hand, Blagg and co-worckers reported during their various SAR studies that the coumarin analogue (I) (Figure 1) which possesses a benzothiophen heterocycle at the C3 position is able to induce the cell death with an IC_{50} of 0.98 µM against SkBr3 cell lines [42]. Inspired by this study combined with the promising activity displayed by 6BrCaQ, we proposed here to design a news series of quinolinone based heterocycle analogues (Figure 1) in which the amide function of 6BrCaQ will be replaced by various heterocycles including benzoxazoles, benzothiazoles, indoles, benzimidazoles and purines in the aim to better understand the SAR in this novel series. In this article the synthesis and the biological evaluation of analogues of type **3, 4** and **5** are described.

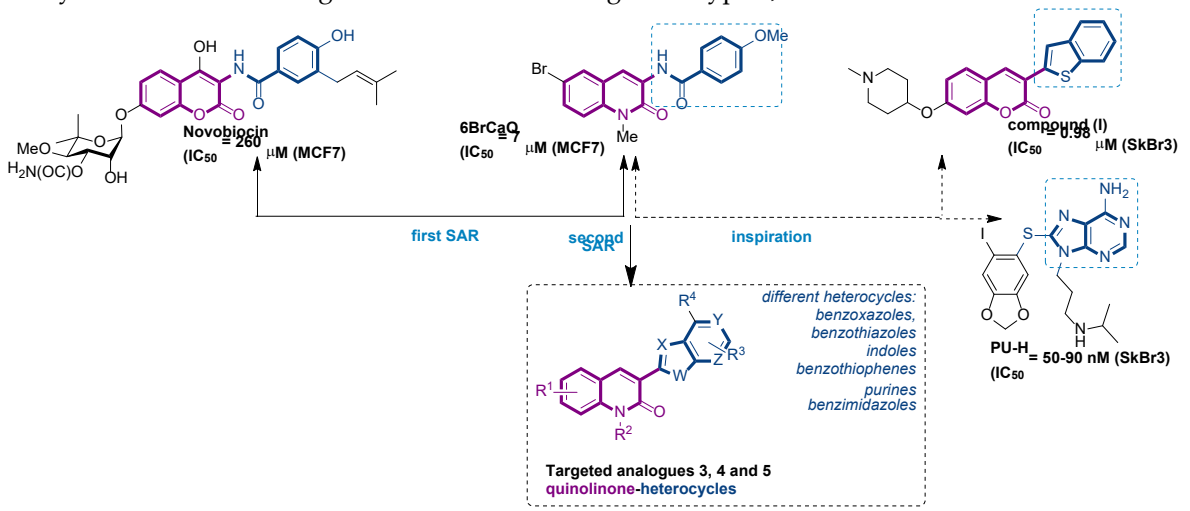

Figure 1. Structure of novobiocin and 6BrCaQ compounds and the approach for the design of targeted compounds **3, 4** and **5**.

2. Results and Discussion

2.1. Chemistry

The first library of compounds targeted is simplified 3-(heteroaryl)quinolin-2(1*H*)-ones **3** (Scheme 1). These analogues were synthesized by the palladium-catalyzed C-H functionalization reaction of 3-bromoquinolin-2-(1*H*)-ones **1** with various azoles according to our previously reported conditions [43]. The reactions take place rapidly in 1,4-dioxane and proceed in good to excellent yields using a bimetallic $Pd(OAc)_2$/CuI as catalysts, PPh_3 as the ligand and Li*O*tBu as the base. Under this convergent protocol compounds **3a-f** were synthesized. These compounds were already reported in reference [43] and were fully characterized and their physical properties can be found also in ref [43]. Various heterocycles could be introduced at the C3-position of the quinolin-2(1*H*)-one nucleus including benzoxazole, benzothiazole, indole, benzimidazole and the SMe-purine (Scheme 1).

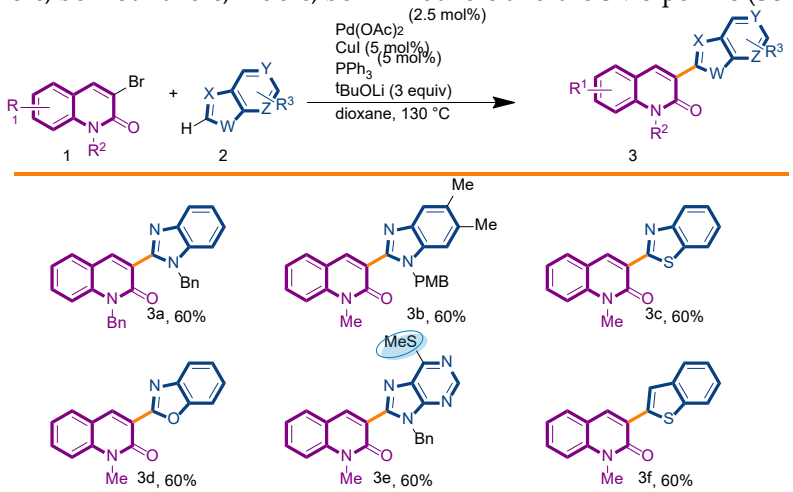

Scheme 1. Synthetic strategy to target 3-(*heteroaryl*)quinolin-2(1*H*)-ones **3**.

In the pursuit of our SAR-study, we were wondering about the possibility of functionalization of the thiomethyl group attached to 6'-position of the purine motif in the derivative **3e**. This motif is found in a series of hsp90 inhibitors such as PU-H71 disclosed in Figure 1. If succeeded, this approach would provide a fast and easy access to a small library of more sophisticated purine-quinolinone analogues. We have rationalized that an additional aromatic group in the molecule **1** would modify the intercalation ability, due to changes in the planarity and in the extension of conjugation.

After a detailed survey about this topic, only few examples of this derivatization of thiopurines were found in the literature. One of the methodologies available to introduce diversity in this particular position is the scarcely explored Liebeskind-Srogl coupling [44], This approach exploits the *pseudo*-halogen character of CH_3S- group (thio-organyl in general) as partner in a Suzuki-like coupling reaction, involving an arylboronic acid under palladium catalysis in the presence of a copper salt [45, 46].

We decided to start our investigations under two approaches: the first one involved the coupling of thiopurinoquinolone **3e** with *p*-methoxyphenyl-boronic acid under $PdDppfCl_2.CH_2Cl_2$ catalysis and conventional heating [47]; while the second method chosen to promote the desired transformation employed $Pd(OAc)_2$ and 1,10-phenanthroline under microwave irradiation [48]. To our delight, both approaches were capable to afford the expected product **4a**, in 61 and 49% yield, respectively (Scheme 2). In order to explore the scope of this synthetic transformation, we decided to use the first method with a sort of arylboronic acids. This election was based on the rational of the electronic and steric effects exerted by the chosen substituents. The reactions proceed smoothly, affording the expected products **4a-h** with yields ranging from 39 to 89% (Scheme 2).

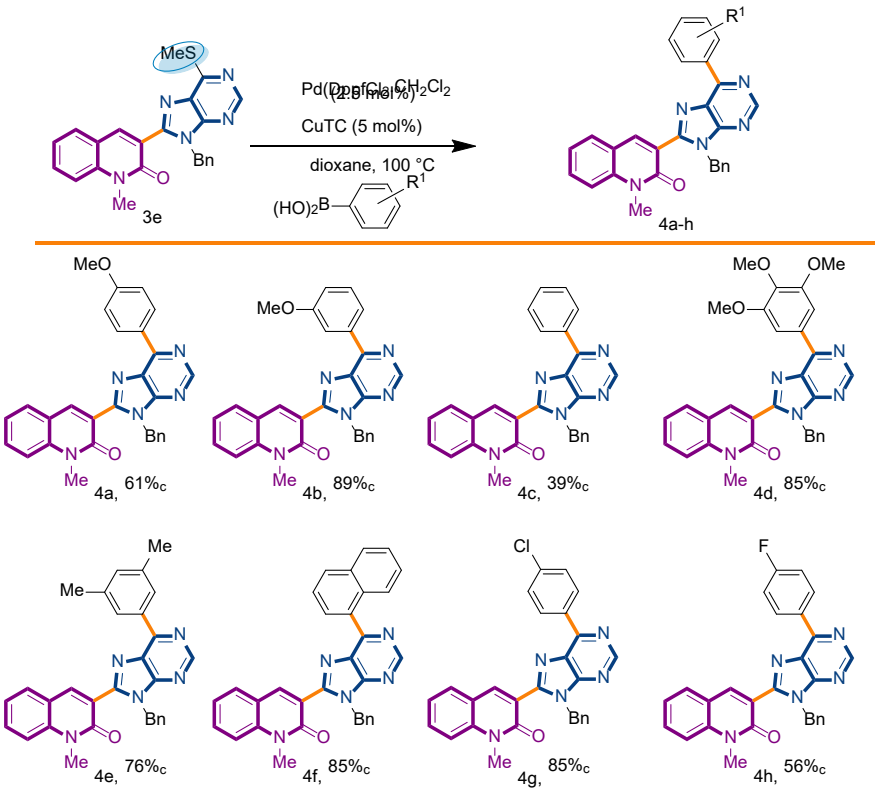

Scheme 2. Synthetic strategy to target 3-(purino)-quinolin-2(1*H*)-ones **4a-h**.

Taking advantage of this synthetic procedure, we decided to examine the scope of Liebeskind-Srogl reaction with anilines (Scheme 3). The introduction of a nitrogen atom at 6'-position of purine ring, would imply its overall transformation into a nucleic acid analogue, *i.e.* an [(*N*-phenyl)adenine] motif. The possibility to have an adenine ring attached to a quinolone nucleus would increase its biological resemblance [49, 50].

It is interesting to denote that this reaction can also be reached by an alternative two-steps procedure involving the initial thioether-sulfone oxidation, followed by a nucleophilic heteroaromatic substitution with the appropriate amine. This protocol has been previously employed by Piguel and coworkers during the synthesis of 6,8,9-purine-derivatives [47]. To the best of our knowledge, the introduction of an amine to the purine ring in 6'-position through a Liebeskind-Srogl reaction has never been reported in the literature.

We started our investigations by adapting the arylsulfide amination protocol described by the group of Murakami [49]. Unfortunately, only degradation of starting material **3e** was detected. Several conditions were assayed including the palladium source, ligand, base and microwave heating [52-54]. To our surprise with a slight modification of the previously used PdDppf.Cl_2/CuTC protocol, the reaction proceeded until completeness, giving the desired product **5a** in 67% yield (Scheme 3). It is important to observe that the presence of CuTC and the Cs_2CO_3 base were mandatory to accomplish the expected transformation.

Under this condition, we succeed to generate the coupling product from 3,4,5-trimethoxyaniline (**5b**, 51%). Unfortunately, however, the reaction of **3e** with aniline, benzyamine, butylamine and pyrrolidine could not be driven to completeness and the expected product could not be separated from the starting material by current chromatographic purification conditions (CC and preparative TLC).

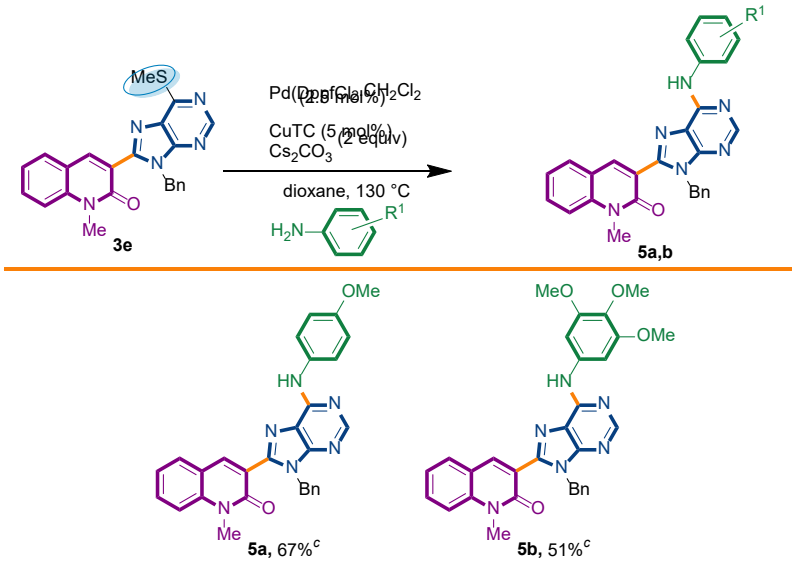

Scheme 3. Synthetic strategy to target 3-adenines-quinolin-2(1*H*)-ones **5a-b.**

Biological evaluation of quinolones analogues

Antiproliferative activity

Upon completion of their syntheses, the *in vitro* activity of quinolone derivatives **3a-f, 4a-h** and **5a,b** was evaluated by their growth-inhibitory potency in three cancer cell lines. At first, the viability of the synthesized compounds was examined with the MDA-MB-231 MCF-7 breast cancer cell line at concentrations of 10 μM, 15 μM and 25 μM. Prostate cancer PC-3 cells and human fetal lung fibroblast MRC-5 cell lines were also subjected to this series of compounds at a unique concentration of 15 μM. The quantification of cell survival in these cell lines was established by using MTS assays after 72 h exposure (Table 1), and GI_{50} values were estimated at the concentration required to produce 50% inhibition (Table 2).

As shown in Table 1, all this series of analogues induced a significant decrease of the cell viability in MDA-MB-231 cells in a concentration depend manner. At 10 μM concentration the viability percentage of MDA-MB-231 cells decreased until less than 47% under **3a** and **5a** exposure (Table 1). In addition, increasing the concentration at 25 μM, analogues **3a, 3b**, **4g** and **4h** affect importantly the growth of MDA-MB-231 cells (~30% survival) clearly demonstrating the bioactivity potential of these compounds.

Then the cytotoxicity activity was examined with two other cancer cell lines: PC-3 cells and human fetal lung fibroblast MRC-5. As shown in the table 1, almost all the reported compounds does not present any effect against MRC-5 cell lines (>82% survival) at 15μM concentration except compounds **4d**, **4e** and **4g** which induce a slight effect in the growth of MRC-5 cells (71% to 79% survival). In contrary, PC-3 cells seems to be more sensitive to these derivatives than MRC-5 cells as we can see in the table 1. Upon exposure of these cell lines at 15 μM concentration, compounds **3b, 3h, 3e, 4e** were able to decrease the cell viability in PC-3 cells until 56%.

Table 1. Cell viability effect of **3a-f**, **4a-h and 5a,b** derivatives against MDA-MB-231, PC-3 and MRC-5 cell lines measured through cell metabolic activity (MTS-based assay).

	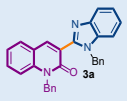	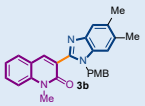	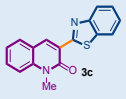	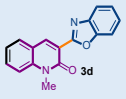	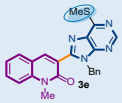	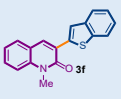
	Cell viability [%][a]					
MDA-MB-231	10 μM 15 μM 25 μM	10 μM 15 μM 25 μM	10 μM 15 μM 25 μM	10 μM 15 μM 25 μM	10 μM 15 μM 25 μM	10μM
	47 47 36	60 60 23	55 72 65	98	73 70 50	98
PC-3 (15 μM)	70	61	61	ND	61	ND
MRC-5 (15 μM)	80	95	88	ND	88	ND
	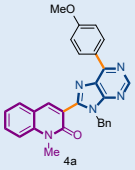	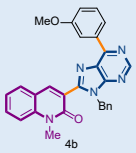	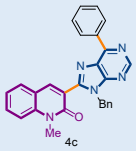	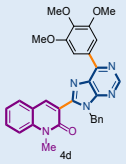	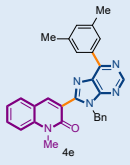	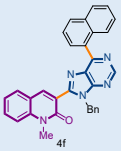
	Cell viability [%][a]					
MDA-MB-231	10 μM 15 μM 25 μM	10 μM 15 μM 25 μM	10 μM 15 μM 25 μM	10 μM 15 μM 25 μM	10 μM 15 μM 25 μM	10μM 15 μM 25 μM
	66 81 87	70 69 61	71 62 35	60 47 55	57 62 50	73 81 92
PC-3 (15 μM)	73	106	97	89	56	88
MRC-5 (15 μM)	94	92	82	70	71	98
	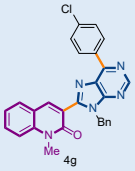	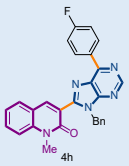	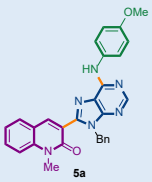	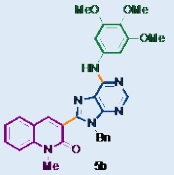	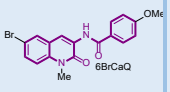	DMSO
	Cell viability [%][a]					
MDA-MB-231	10 μM 15 μM 25 μM	10 μM 15 μM 25 μM	10 μM 15 μM 25 μM	10 μM 15 μM 25 μM	10 μM	100
	56 57 27	55 42 17	62 63 69	44 55 61	76	
PC-3 (15 μM)	91	97	87	88	ND	100
MRC-5 (15 μM)	79	84	91	81	ND	100

Cell viability:

	< 69%
	70% to 80%
	> 80%

[a] Value of the anti-proliferative or cytotoxic effect measured by MTS assay (% of viable cells compared to untreated cells 100%) of analogues **3a-f, 4a-h** and **5a,b** derivatives against MDA-MB-231, PC-3 and MCR-5-7 cell lines at the indicated concentrations. ND: not determined.

179 Then, the growth inhibitory activities against PC-3 prostate cancer cell line were measured for
180 the selected 3-heteroaryl-quinolin-2(1*H*)-one derivatives **3a-e**. All the compounds shown in Table 2
181 display an estimated GI_{50} ranging between 28 μM to 48 μM. Of the selected derivatives, **3b** showed a
182 significant ability to inhibit cell growth and was the most cytotoxic (GI_{50} = 28 μM) against the PC-3
183 prostate cancer cell lines.
184

Table 2. GI_{50} (μM) values for anti-proliferative effects of selected compounds **3a-e**[a]

compound	PC-3
6Br-CaQ	10
3a	48
3b	28
3c	37
3e	38

[a] GI_{50} is the concentration of compound needed to reduce cell growth by 50% following 72 h cell treatment with the tested drug.

185

186 To provide additional evidence that the growth inhibitory activity manifested by the derivatives,
187 the most active compounds **3a-e**, **4e** and **5b** were evaluated for their ability to induce degradation of
188 Hsp90-dependent client protein Cdk4, the most widely studied molecular signatures indicative of
189 Hsp90 blockade.
190 As depicted in Figure 2, the cyclin-dependant kinase CdK4 was degraded following treatment
191 with **3a-e**, **4e** and **5b**. The GAPDH protein was not affected by the tested compounds, indicating
192 selective degradation of hsp90-dependent clients. CDK-4 level was more decreased by compounds
193 **3b** and **4e** at concentration of 15 μM. One can note that the anti-proliferative activity of **3b** (IC_{50} = 28
194 μM, Table 2) and **4e** correlate well with the concentration needed to induce Hsp90/CDK-4 client
195 protein degradation.
196 Hsp90 N-terminal inhibitors induce a Heat-shock-response by releasing a transcription factor
197 (HSF1) of the genes of Hsp27, Hsp70 and Hsp90. This increase in transcription leads to opposition to
198 apoptosis and, thus, to resistance to treatment.
199 This is important to check that the levels of these proteins are not increasing with our
200 compounds. We showed by western blot that **3a-e**, **4e** and **5b** stabilizes the levels of Hsp90 and Hsp70
201 without triggering the HSR. This result was already observed with 6-BrCaQ in PC-3 cell lines as we
202 reported previously: liposomal 6-BrCaQ stabilized levels of Hsp70 and decreased level of Hsp90 [40].
203
204

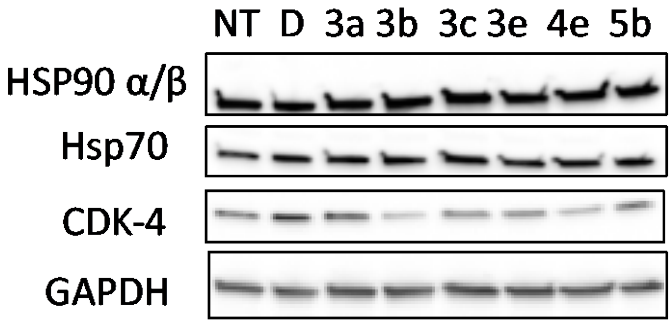

Figure 2. Effects of quinolone analogues **3a-e, 4e** and **5b** on HSP90 machinery protein levels and on CDK-4 stability. PC-3 cells were grown and exposed to Hsp90 inhibitors (**3a-e, 4e** and **5b**, 15μM) as described in Experimental section for 72 h and cell lysates were analyzed by Western blotting with regard to the levels of CDK-4, Hsp90α/β and Hsp70. NT corresponds to untreated cells; D, DMSO-treated cells were used as controls, GADPH level is used for control in protein loading on gels.

Conclusion

In summary, we have designed and synthesized a new series of 3-heteroaryl-quinolin-2(1*H*)-one derivatives as potential Hsp90 inhibitors. During this study, we developed a Pd-catalyzed Liebeskind-Srogl cross-coupling reaction between SMe-containing quinolinyl-purine derivative and various aryl boronic acids. We reported also for the first time, that anilines may be used as nucleophilic partners during this coupling. From these SAR studies, **3a-e**, **4e** and **5b** were found to display the most stronger cell viability effect against MDA-MB 231 and PC-3 cancer cell lines. In addition compounds **3b** and **4e** were found to be able to induce a significant decrease of CDK-1 client protein and stabilize the levels of Hsp90 and Hsp70 without triggering the HSR response.

3. Materials and Methods

3.1. General Experimental Methods

The compounds were all identified by the usual physical methods, that were ^{1}H -NMR, ^{13}C-NMR, IR, and HRMS (ESI). The ^{1}H and ^{13}C NMR spectroscopic data were recorded on a Bruker Avance 300 FT-NMR (300.13 MHz for ^{1}H NMR and 75.48 MHz for ^{13}C NMR). ^{1}H and ^{13}C NMR spectra were measured in $CDCl_3$ unless otherwise stated. ^{1}H chemical shifts are reported in ppm using tetramethylsilane (TMS) as internal standard. The following abbreviations are used: m (multiplet), s (singlet), bs (broad singlet), d (doublet), t (triplet), dd (doublet of doublet), td (triplet of doublet), q (quadruplet), qui (quintuplet), sex (sextuplet). ^{13}C NMR chemical shifts are reported in ppm from the central peak of deuterochloroform (77.1). IR spectra were measured on a Bruker Vector 22 spectrophotometer [neat, ATR] and are reported in wave numbers (cm^{-1}). High resolution mass spectra (HRMS) were recorded by direct infusion in a mass spectrometer LCT Premier/XE (Waters).

General Methods: All glassware was oven-dried at 140°C and all reactions were conducted under dry argon atmosphere. The solvents cyclohexane, ethyl acetate and MeOH for chromatography were purchased to Aldrich and were used as received. The reactions were monitored by TLC run in cyclohexane/EtOAc mixtures. The plates were visualized by UV light (254 and 365 nm) and immersed into a solution of phosphomolybdic acid in ethanol, and carefully heated to improve selectivity.

Preparative TLC was performed on a 2.0 mm thickness Merck pre-coated silica gel PLC plates. Merck silica gel 60 (230–400 mesh) was used for column chromatography employing cyclohexane/EtOAc polarity gradient techniques, under positive pressure. Melting points were recorded on a Büchi B-450 apparatus and are uncorrected.

3.2. General procedure for the Liebeskind-Srogl coupling of 3-(6-methylthiopurine)-2-quinolone (3e) and boronic acids:

In a reaction tube under argon atmosphere were mixed quinolone **3e** (1 equiv.), the boronic acid (2.0 equiv.), $PdDppfCl_2.CH_2Cl_2$ (0.02 equiv.) and CuTC (2 equiv.) in dry dioxane (10 mL/mmol). The tube was sealed and placed into a pre-heated oil bath at 80-90 °C until reaction completeness (4-8 h) ascertained by TLC. The volatiles were removed in the rotavapor and the crude material was purified by column chromatography or preparative TLC.

3-[9-benzyl-6-(4-methoxyphenyl)-9*H*-purin-8-yl]-1-methylquinolin-2(1*H*)-one (**4a**): 27 mg, 0.056 mmol, Yield 61 %. Colorless oil. R_f = 0.67 (C_6H_{12}/AcOEt 50%). IR (ATR-diamond, ν): 2963, 1649, 1642, 1598, 1578, 1512, 1453, 1413, 1322, 1292, 1251, 1174, 1103, 1028, 1013, 873, 846, 804, 750, 734, 699 cm^{-1}. ^1H NMR δ: 3.84 (s, 3H, NCH_3), 3.90 (s, 3H, $ArOCH_3$), 5.74 (s, 2H, NCH_2Ph), 7.00-7.12 (m, 7H, Bn, $ArOCH_3$), 7.28 (dt, *J* = 7.9, 0.7 Hz, 1H), 7.42 (d, *J* = 8.7 Hz, 1H), 7.57 (dd, *J* = 7.9, 1.5 Hz, 1H), 7.66 (dd, *J* = 8.3, 0.7 Hz, 1H), 8.05 (s, 1H, H-4), 8.87 (d, *J* = 9.0 Hz, 2H, $ArOCH_3$), 9.01 (s, 1H, H-4'). ^{13}C NMR δ: 30.1, 47.1, 55.4, 113.5, 114.1, 114.3, 119.7, 122.8, 123.2, 127.4, 128.3, 128.5, 129.9, 130.3, 131.7, 132.4, 136.4, 140.6, 143.2, 151.9, 152.3, 153.8, 154.1, 160.1, 162.0. HRMS *m*/*z* calcd for $C_{29}H_{25}N_6O_2$: 489.2039 $[M + H]^+$, found: 489.2030.

3-[9-benzyl-6-(3-methoxyphenyl)-9*H*-purin-8-yl]-1-methylquinolin-2(1*H*)-one (**4b**): 47 mg, 0.099 mmol, Yield 89 %. Colorless oil. R_f = 0.29 (C_6H_{12}/AcOEt 50%). IR (ATR-diamond, ν): 3250, 1646, 1461, 1323, 1218, 1161, 1071, 954, 791 cm^{-1}. ^1H NMR δ (*d*$_6$-acetone): 3.87 (s, 3H, NCH_3), 3.91 (s, 3H, OCH_3), 5.76 (s, 2H, NCH_2Ph), 7.07-7.15 (m, 6H, Bn, $ArOCH_3$), 7.35 (dt, *J* = 7.9, 0.9 Hz, 1H), 7.49 (d, *J* = 7.9 Hz, 1H), 7.66 (d, J= 8.3 Hz, 1H), 7.77 (dt, *J* = 7.9, 1.5 Hz, 1H), 7.81 (d, *J* = 7.9 Hz, 1H), 8.29 (s, 1H), 8.64-8.67 (m, 2H, $ArOCH_3$), 9.01 (s, 1H, H-4'). ^{13}C NMR δ (*d*$_6$-acetone): 30.2, 47.6, 55.7, 115.7, 117.5, 120.5, 123.2, 123.5, 128.3, 128.4, 129.3, 130.3, 130.8, 133.3, 143.9, 153.7, 160.6, 160.8. HRMS *m*/*z* calcd for $C_{29}H_{24}N_5O_2$: 474.1930 $[M + H]^+$, found: 474.1937.

3-(9-benzyl-6-phenyl-9*H*-purin-8-yl)-1-methylquinolin-2(1*H*)-one (**4c**): 10 mg, 0.024 mmol, Yield 39 %. Colorless oil. R_f = 0.52 (C_6H_{12}/AcOEt 50%). IR (ATR-diamond, ν): 3060, 2931, 1641, 1586, 1466, 1331, 1298, 1166, 954, 768, 668 cm^{-1}. ^1H NMR δ: 3.84 (s, 3H, NCH_3), 5.74 (s, 2H, NCH_2Ph), 7.00-7.13 (m, 5H, Bn), 7.29 (t, *J* = 8.1 Hz, 1H), 7.43 (d, *J* = 8.7 Hz, 1H), 7.48-7.62 (m, 8H), 7.67 (dd, *J* = 8.7, 1.5 Hz, 2H), 8.05 (s, 1H, H-4), 8.25 (d, *J* = 6.8 Hz, 1H, H-4''), 8.81 (dd, *J* = 8.3, 1.9 Hz, 2H, H-2'',6''), 9.08 (s, 1H, H-4'). ^{13}C NMR δ: 30.1, 47.1, 114.3, 119.7, 122.9, 123.1, 127.4, 127.7, 127.8, 128.0, 128.5, 128.7, 129.9, 130.7, 130.9, 132.4, 132.7, 133.2, 133.5, 135.9, 136.4, 140.6, 143.3, 152.2, 152.5, 154.3, 154.4, 160.1. HRMS *m*/*z* calcd for $C_{28}H_{21}N_5ONa$: 466.1644 $[M + Na]^+$, found: 466.1646.

3-[9-benzyl-6-(3,4,5-trimethoxyphenyl)-9*H*-purin-8-yl]-1-methylquinolin-2(1*H*)-one (**4d**): 24 mg, 0.053 mmol, Yield 85 %. Colorless oil. R_f = 0.28 (C_6H_{12}/AcOEt 50%). IR (ATR-diamond, ν): 2939, 2836,

1641, 1505, 1444, 1346, 1217, 11241072, 1002, 952, 858, 723, 697 cm^{-1}. ^1H NMR δ: 3.84 (s, 3H, NCH_3), 3.93 (s, 3H, OCH_3), 3.938 (s, 6H, OCH_3), 5.72 (s, 2H, NCH_2Ph), 6.96-7.02 (m, 2H, Bn), 7.07-7.11 (m, 3H, Bn), 7.28 (t, *J* = 7.4 Hz, 1H), 7.44 (d, *J* = 8.5 Hz, 1H), 7.57 (d, *J* = 7.9 Hz, 1H), 7.68 (dt, *J* = 7.4, 1.5 Hz, 1H) 8.03 (s, 1H), 8.25 (s, 2H, $ArOCH_3$), 9.03 (s, 1H, H-4'). ^{13}C NMR δ: 30.1, 47.1, 56.3, 61.0, 107.3, 114.4, 119.7, 122.9, 123.4, 127.4, 127.7, 128.5, 129.9, 130.8, 131.3, 132.4, 136.4, 140.6, 143.0, 152.0, 153.3, 153.7, 154.3, 160.1. HRMS *m*/*z* calcd for $C_{31}H_{28}N_5O_4$: 534.2141 $[M + H]^+$, found: 534.2148.

3-[9-benzyl-6-(3,5-dimethylphenyl)-9*H*-purin-8-yl]-1-methylquinolin-2(1*H*)-one (**4e**): 19 mg, 0.054 mmol, Yield 76 %. Colorless oil. R_f = 0.61 (C_6H_{12}/AcOEt 50%). IR (ATR-diamond, ν): 3037, 2910, 1646, 1582, 1447, 1322, 1216, 1117, 1073, 955, 863, 725 cm^{-1}. ^1H NMR δ: 3.83 (s, 3H, NCH_3), 5.73 (s, 2H, NCH_2Ph), 6.98-7.01 (m, 2H, Bn), 7.07-7.12 (m, 3H, Bn), 7.14 (s, 1H, $ArCH_3$), 7.28 (t, *J* = 7.4 Hz, 1H), 7.43 (d, *J* = 8.5 Hz, 1H), 7.59 (d, *J* = 7.7 Hz, 1H), 7.67 (t, *J* = 7.4 Hz, 1H) 8.07 (s, 1H), 8.42 (s, 2H, $ArCH_3$), 9.06 (s, 1H, H-4'). ^{13}C NMR δ: 21.5, 30.1, 47.1, 114.3, 119.7, 122.8, 123.2, 127.4, 127.6, 127.7, 128.5, 130.0, 130.9, 132.4, 132.7, 135.7, 136.4, 138.2, 140.6, 143.3, 152.1, 152.4, 154.2, 154.8, 160.1. HRMS *m*/z calcd for $C_{30}H_{26}N_5O$: 472.2137 $[M + H]^+$, found: 472.2139.

3-[9-benzyl-6-(naphthalen-2-yl)-9*H*-purin-8-yl]-1-methylquinolin-2(1*H*)-one (**4f**): 21 mg, 0.059 mmol, Yield 85 %. Colorless oil. R_f = 0.61 (C_6H_{12}/AcOEt 50%). IR (ATR-diamond, ν): 3067, 1642, 1570, 1446, 1320, 1276, 1168, 920, 847, 754, 696 cm^{-1}. ^1H NMR δ: 3.85 (s, 3H, NCH_3), 5.76 (s, 2H, NCH_2Ph), 7.02-7.12 (m, 5H, Bn), 7.29 (t, *J* = 8.1 Hz, 1H), 7.43 (d, *J* = 8.5 Hz, 1H), 7.48-7.56 (m, 2H), 7.60 (d, *J* = 7.3 Hz, 1H), 7.67 (d, *J* = 7.7 Hz, 1H), 7.88 (d, *J* = 8.7 Hz, 1H), 7.99 (d, *J* = 8.7 Hz, 1H), 8.05 (d, *J* = 7.3 Hz, 1H), 8.11 (s, 1H, H-4), 8.97 (d, *J* = 8.3 Hz, 1H, Naphthyl), 9.12 (s, 1H, H-4'), 9.46 (s, 1H, Naphthyl). ^{13}C NMR δ: 30.1, 47.2, 114.3, 119.7, 122.9, 123.2, 126.2, 126.3, 127.3, 127.5, 127.7**0**, 127,7**4**, 128.2, 128.5, 123.0, 130.8, 131.2, 132.4, 133.3, 133.4, 133.6, 134.6, 136.4, 140.6, 143.4, 152.3, 152.5, 154.1, 154.4, 160.1. HRMS *m*/*z* calcd for $C_{32}H_{24}N_5O$: 494.1981 $[M + H]^+$, found: 494.1976.

3-[9-benzyl-6-(4-chlorophenyl)-9*H*-purin-8-yl]-1-methylquinolin-2(1*H*)-one (**4g**): 34 mg, 0.083 mmol, Yield 85 %. Colorless solid, m.p.: 202-203 °C (CH_2Cl_2/MeOH). R_f = 0.65 (C_6H_{12}/AcOEt 50%). IR (ATR-diamond, ν): 3044, 2928, 1641, 1582, 1492, 1381, 1298, 1177, 1089, 953, 803, 736, 720 cm^{-1}. ^1H NMR δ: 3.85 (s, 3H, NCH_3), 5.73 (s, 2H, NCH_2Ph), 6.99-7.03 (m, 2H, Bn), 7.07-7.12 (m, 3H, Bn), 7.30 (dt, *J* = 7.9, 0.7 Hz, 1H), 7.44 (d, *J* = 8.5 Hz, 1H), 7.51 (d, *J* = 8.5 Hz, 2H, ArCl), 7.69 (dd, *J* = 8.7, 1.7 Hz, 1H), 8.04 (s, 1H), 8.85 (d, *J* = 8.5 Hz, 2H, ArCl), 9.06 (s, 1H, H-4'). ^{13}C NMR δ: 30.1, 47.2, 114.3, 119.7, 122.9, 123.0, 127.5, 127.8, 128.9, 130.0, 130.8, 131.2, 132.5, 134.4, 136.3, 137.0, 140.6, 143.3, 152.4, 152.9, 154.4, 160.0. HRMS *m*/*z* calcd for $C_{28}H_{21}N_5OCl$: 478.1435 $[M + H]^+$, found: 478.1440.

3-[9-benzyl-6-(4-fluorophenyl)-9*H*-purin-8-yl]-1-methylquinolin-2(1*H*)-one (**4h**): 22 mg, 0.047 mmol, Yield 56 %. Colorless oil. R_f = 0.57 (C_6H_{12}/AcOEt 50%). IR (ATR-diamond, ν): 3058, 2958, 1642, 1569, 1463, 1320, 1297, 1159, 1070, 952, 847, 724, 698 cm^{-1}. ^1H NMR δ: 3.63 (s, 3H, NCH_3), 5.65 (s, 2H, NCH_2Ph), 6.91-6.94 (m, 2H, Bn), 6.99-7.05 (m, 3H, Bn), 7.14 (t, *J* = 8.9 Hz, 2H, ArF), 7.22 (t, *J* = 7.9 Hz, 1H), 7.36 (d, *J* = 8.5 Hz, 1H), 7.51 (dd, *J* = 7.9, 1.3 Hz, 1H), 7.61 (dt, *J* = 8.5, 1.3Hz, 1H), 7.97 (s, 1H, H-4), 8.84 (dd, *J* = 8.9, 5.6 Hz, 1H, ArF), 8.97 (s, 1H, H-4'). ^{13}C NMR δ: 30.1, 47.1, 67.1 114.3, 115.7 (d, $^2J_{C-F}$ = 21.6 Hz), 119.7, 122.9, 123.1, 127.5, 127.8, 128.5, 130.0, 132.1 (d, $^3J_{C-F}$ = 8.3 Hz), 136.3, 140.6, 143.3, 152.3, 152.5, 153.0, 154.3, 160.1, 164.5 (d, $^1J_{C-F}$ = 249.8 Hz). HRMS *m*/*z* calcd for $C_{28}H_{20}N_5OFNa$: 484.1550 $[M + Na]^+$, found: 484.1552.

3.3. Procedure for the Liebeskind-Srogl coupling of 3-(6-methylthiopurine)-2-quinolone (3e) and anilines:

In a reaction tube equipped with a stirring bar under argon atmosphere were admixed quinolone **3e** (1 equiv.), the appropriate aniline (2.0 equiv.), PdDppfCl$_2$.CH$_2$Cl$_2$ (0.1 equiv.), Ph$_3$P (0.2 equiv.), Cs$_2$CO$_3$ (2.0 equiv.) and CuTC (2 equiv.) in dry dioxane (20 mL/mmol). The tube was sealed and poured into a pre-heated oil bath at 130 °C until consumption of quinolone **1**, monitored by TLC (15-18 hs). The volatiles were removed in the rotavapor and the crude material was suspended with AcOEt, filtered through a short pad of cotton, concentrated under vacuum and the remaining solid was purified by preparative TLC (2 × C$_6$H$_{12}$/AcOEt 50%).

3-{9-benzyl-6-[(4-methoxyphenyl)amino]-9*H*-purin-8-yl}-1-methylquinolin-2(1*H*)-one (**5a**): 20 mg, 0.039 mmol, Yield 67 %. Yellowish oil. R_f = 0.36 (2 × C$_6$H$_{12}$/AcOEt 50%). IR (ATR-diamond, ν): 3283, 3038, 2928, 2847, 1641, 1588, 1573, 1461, 1380, 1241, 1180, 1087, 953, 829, 755, 697 cm^{-1}. ^{1}H NMR δ: 3.74 (s, 3H, NCH$_3$), 3.75 (s, 3H, OCH$_3$), 5.54 (s, 2H, NCH$_2$Ph), 6.92 (d, *J* = 8.9 Hz, 2H, Ar), 6.99-7.02 (m, 2H, Bn), 7.09-7.13 (m, 3H, Bn), 7.26 (t, *J* = 8.2 Hz, 1H, H-6), 7.41 (d, *J* = 8.5 Hz, 1H, H-8), 7.48 (d, *J* = 7.7 Hz, 1H, H-5), 7.62-7.68 (m, 3H, H-7, ArOCH$_3$), 7.71 (s$_b$, 1H, N*H*) 7.86 (s, 1H, H-4), 8.55 (s, 1H, H-4'). ^{13}C NMR δ: 30.0, 47.1, 55.5, 114.3, 119.6, 119.9, 122.5, 122.8, 123.0, 127.4, 127.9, 128.5, 129.8, 131.7, 132.2, 136.6, 140.5, 142.4, 147.9, 151.2, 152.2, 153.2, 156.1, 160.1. HRMS *m*/*z* calcd for C$_{29}$H$_{25}$N$_6$O$_2$: 489.2039 [M + H]$^+$, found: 489.2030.

3-{9-benzyl-6-[(3,4,5-trimethoxyphenyl)amino]-9*H*-purin-8-yl}-1-methylquinolin-2(1*H*)-one (**5b**): 14 mg, 0.025 mmol, Yield 51 %. Yellowish oil. R_f = 0.18 (3 × C$_6$H$_{12}$/AcOEt 50%). IR (ATR-diamond, ν): 3296, 3039, 2933, 2834, 1642, 1588, 1463, 1323, 1126, 1088, 954, 697 cm^{-1}. ^{1}H NMR δ: 3.82 (s, 3H, NCH$_3$), 3.83 (s, 3H, OCH$_3$), 3.87 (s, 6H, OCH$_3$), 5.63 (s, 2H, N-CH$_2$Ph), 6.99-7.02 (m, 2H, Bn), 7.09-7.14 (m, 3H, Bn), 7.16 [s, 2H, Ar(OCH$_3$)$_3$], 7.27 (t, *J* = 7.4 Hz, 1H, H-6), 7.42 (d, *J* = 8.5 Hz, 1H, H-8), 7.49 (d, *J* = 7.2 Hz, 1H, H-5), 7.66 (t, *J* = 7.9 Hz, 1H, H-7), 7.87 (s$_b$, 1H, NH), 8.31 (s, 1H, H-4), 8.59 (s, 1H, H-10). ^{13}C NMR δ: 30.1, 47.1, 56.1, 61.0, 98.0, 114.3, 119.6, 119.8, 122.8, 122.8, 127.4, 127.7, 128.5, 129.8, 132.3, 135.1, 136.5, 140.5, 142.5, 148.2, 151.9, 153.1, 153.3, 160.2. HRMS *m*/*z* calcd for C$_{31}$H$_{29}$N$_6$O$_4$: 549.2250 [M + H]$^+$, found: 549.2250.

3.4. Materials and Methods for Cell culture and Western blot analysis

MDA-MB-231 cells were grown in L15 supplemented with 15% serum, 2 mM glutamine and 22mM sodium bicarbonate in the presence of Penicillin/Streptomycin antibiotic mixture. PC-3 cells were cultured in RPMI 1640 supplemented with 10% serum and 2 mM glutamine in the presence of Penicillin/Streptomycin antibiotic mixture. MRC-5 cells were cultured in EMEM supplemented with 10% serum and 2 mM glutamine in the presence of Penicillin/Streptomycin antibiotic mixture.

Cells were treated for 72h with 10, 15 and 25 μM of the selected substances. Control cells were treated with the equivalent in DMSO.

Cell survival was assessed using the CellTiter Aqueous One Proliferation assay: 2500 or 5000 cells per well were seeded in 96-well plates in 100 μL. At the end of the treatment, 20 μL of reagent was added and absorbance readings were taken at 492 nm on a 96-well plate reader after 3 h of contact (on average).

For protein expression analysis, cells were seeded at a rate of $0.75.10^6$ cells on a 25 cm^2 surface. At the end of the treatment the cells were washed and lysed with RIPA buffer (SIGMA) to which protease inhibitors (SIGMA) were added. After 30 minutes of lysis on ice, the samples were centrifuged (3500 rpm, 10 min) and stored at -20°C. Total protein concentration was obtained using the Bio-rad Protein Assay reagent (Bio-Rad Laboratories). Thirty μg of protein (denatured in the presence of Laemmli buffer, sample buffer from Bio-Rad) was plated on a 4-15% pre-cast acrylamide gel (Bio-Rad) and subjected to SDS-PAGE (150 V, 1 h) and PVDF membrane transfer (100 V, 45 min). Immunorevelation was performed as follows: 1 h saturation of the membrane with TBS-Tween (0.1%)-5% skim milk followed by overnight incubation in primary antibody solution (See table below). After 1 h of washing in 0.1% TBS-Tween, the membranes were contacted with the second Horse Radish Pexoxydase-coupled antibody. Detection of the chemiluminescence signal (SuperSignal Pierce reagent) was performed using the ChemiBis reader (DNR).

Primary antibody	Dilution	Secondary antibody (from Santa-Cruz)	Dilution
Anti-Hsp90 α/β (H-114) (Santa-Cruz)	**1/500**	**Anti-rabbit**	**1/10000**
Anti-Hsp70 (Santa-Cruz)	**1/500**	**Anti-mouse**	**1/3000**
Anti-CDK-4 (C-22) (Santa-Cruz)	**1/500**	**Anti-rabbit**	**1/10000**
Anti-GAPDH (SIGMA)	**1/5000**	**Anti-rabbit**	**1/10000**

Supplementary Materials: The following are available online at www.mdpi.com/link: spectra for all synthesized compounds.

Acknowledgments: Authors acknowledge the support of this project by CNRS, University Paris Paris Sacaly. ELL also thanks CONICET for the fellowship and Agencia Nacional de Promoción Científica y Tecnológica (ANPCyT, PICT 2018-01933).

Author Contributions: SM and MA conceived and designed the experiments; ELL developed and performed the synthetic approach for the synthesis of the 6BrCaQ analogues; AB and FS performed the biological evaluations under the supervision of JV-G. ELL, AB, FS, MA, JV-G, and SM wrote the paper. All authors have read and agreed to the published version of the manuscript.

Conflicts of Interest: The authors declare no conflict of interest.

References

1. Messaoudi, S.; Peyrat, J.-F.; Brion, J.-D.; Alami, M. Recent advances in Hsp90 inhibitors as antitumor agents. *Anticancer Agents Med. Chem.* **2008**, *8*, 761–782.
2. Sgobba, M.; Rastelli, G. Structure-based and *in silico* design of Hsp90 inhibitors. *ChemMedChem.* **2009**, *4*, 1399–1409.

3. Janin, Y.L. ATPase inhibitors of heat-shock protein 90, second season. *Drug Discov. Today* **2010**, *15*, 342–353.
4. Messaoudi, S.; Peyrat, J.-F.; Brion, J.-D.; Alami, M. Heat-shock protein 90 inhibitors as antitumor agents: A survey of the literature from 2005 to 2010. *Expert. Op. Th. Pat.* **2011**, *21*, 1501–1542.
5. Messaoudi, S.; Peyrat, J.-F.; Brion, J.-D.; Alami, M. Recent advances in hsp90 inhibitors as antitumor agents. In *Advances in anti-cancer agents in medicinal chemistry*. 1st ed.; Prudhomme, M. Ed.; Bentham Sciences Publishers, Oak Park, USA, 2013, Volume 1, pp. 107–183.
6. Neckers, L. Heat shock protein 90: the cancer chaperone. *J. Biosci.* **2007**, *32*, 517–530.
7. Amolins, M.W.; Blagg, B.S.J. Natural product inhibitors of Hsp90: potential leads for drug discovery. *Mini Rev. Med. Chem.* **2009**, *9*, 140–152.
8. Maloney, A.; Workman, P. HSP90 as a new therapeutic target for cancer therapy: the story unfolds. *Expert Opin. Biol. Th.* **2002**, *2*, 3–24.
9. Whitesell, L.; Lindquist, S.-L. HSP90 and the chaperoning of cancer. *Nat. Rev. Cancer*. **2005**, *5*, 761–772.
10. Zhang, H.; Burrows, F. Targeting multiple signal transduction pathways through inhibition of Hsp90. *J. Mol. Med.* **2004**, *82*, 488–499.
11. Blagg, B.S.J.; Kerr, T.D. Hsp90 inhibitors: small molecules that transform the Hsp90 protein folding machinery into a catalyst for protein degradation. *Med. Res. Rev.* **2006**, *26*, 310–338.
12. Chène, P. ATPases as drug targets: learning from their structure. *Nat. Rev. Drug Discov.* **2002**, *1*, 665–673.
13. Taldone, T,; Sun, W.; Chiosis, G. Discovery and development of heat shock protein 90 inhibitors. *Bioorg. Med. Chem.* **2009**, *17*, 2225–2235.
14. Taldone, T.; Gozman, A.; Maharaj, R.; Chiosis, G. Targeting Hsp90: small-molecule inhibitors and their clinical development. *Curr. Opin. Pharmacol.* **2008**, *8*, 370–374. https://doi.org/10.1016/j.coph.2008.06.015.
15. Mahalingam, D.; Swords, R.; Carew, J.S.; Nawrocki, S.T.; Bhalla, K.; Giles, F.J. Targeting Hsp90 for cancer therapy. *Br. J. Cancer* **2009**, *100*, 1523–1529.
16. Panaretou, B.; Prodromou, C.; Roe, S.M.; O'Brien, R.; Ladbury, J.E.; Piper, P.W.; Pearl, L.H. ATP binding and hydrolysis are essential to the function of the Hsp90 molecular chaperone in vivo. *EMBO J.* **1998**, *17*, 4829–4836.
17. Clarke, P.A.; Hostein, I.; Banerji, U.; Stefano, F.D.; Maloney, A.; Walton, M.; Judson, I.; Workman, P. Gene expression profiling of human colon cancer cells following inhibition of signal transduction by 17-allylamino-17-demethoxygeldanamycin, an inhibitor of the Hsp90 molecular chaperone. *Oncogene* **2000**, *19*, 4125–4133.
18. Erlichman, C. Tanespimycin: the opportunities and challenges of targeting heat shock protein 90. *Expert Opin. Investig. Drugs* **2009**, *18*, 861–868.
19. McCollum, A.K.; Teneyck, C.J.; Sauer, B.M.; Toft, D.O.; Erlichman, C. Up-regulation of heat shock protein 27 induces resistance to 17-allylamino-demethoxygeldanamycin through a glutathione-mediated mechanism. *Cancer Res.* **2006**, *66*, 10967–10975.
20. Demidenko, Z.N.; Vivo, C.; Halicka, H.D.; Li, C.J.; Bhalla, K.; Broude, E.V.; Blagosklonny, M.V. Pharmacological induction of Hsp70 protects apoptosis-prone cells from doxorubicin: comparison with caspase-inhibitor- and cycle-arrest- mediated cytoprotection. *Cell. Death Differ.* **2006**, *13*, 1434–1441.
21. Gabai, V.L.; Budagova, K.R.; Sherman, M.Y. Increased expression of the major heat shock protein Hsp72 in human prostate carcinoma cells is dispensable for their viability but confers resistance to a variety of anticancer agents. *Oncogene* **2005**, *24*, 3328–3338.

22. Pocaly, M.; Lagarde, V.; Etienne, G.; Ribeil, J.A.; Claverol, S.; Bonneu, M.; Moreau-Gaudry, F.; Guyonnet-Duperat, V.; Hermine, O.; Melo, J.V.; Dupouy, M.; Turcq, B.; Mahon, F.X.; Pasquet, J.M. Overexpression of the heat-shock protein 70 is associated to imatinib resistance in chronic myeloid leukemia. *Leukemia* **2007**, *21*, 93–101.
23. Wang, R.E. Targeting heat shock proteins 70/90 and proteasome for cancer therapy. *Curr. Med. Chem.* **2011**, *18*, 4250–4264.
24. Wang, H.; Tan, M.S.; Lu, R.C.; Yu, J.T.; Tan, L. Heat shock proteins at the crossroads between cancer and Alzheimer's disease. *Biomed. Res. Int.* **2014**, 239164.
25. Murphy, M.E. The Hsp70 family and cancer. *Carcinogenesis* **2013**, *34*, 1181–1188.
26. Donnelly, A.; Blagg, B.S.J. Novobiocin and additional inhibitors of the Hsp90 C-terminal nucleotide-binding pocket. *Curr. Med. Chem.* **2008**, *15*, 2702–2717.
27. Eskew, J.D.; Sadikot, T.; Morales, P.; Duren, A.; Dunwiddie, I.; Swink, M.; Zhang, X.; Hembruff, S.; Donnelly, A.; Rajewski, R.A.; Blagg, B.S.J.; Manjarrez, J.R.; Matts, R.L.; Holzbeierlein, J.M.; Vielhauer, G.A. Development and characterization of a novel C-terminal inhibitor of Hsp90 in androgen dependent and independent prostate cancer cells. *BMC Cancer* **2011**, *11*, 468.
28. Buckton, K.; Wahyudi, H.; McAlpine, S.R. The first report of direct inhibitors that target the C-terminal MEEVD region on heat shock protein 90 L. *Chem. Commun.* **2016**, *52*, 501–504.
29. Burlison, J.A.; Avila, C.; Vielhauer, G.; Lubbers, D.J.; Holzbeierlein, J.; Blagg, B.S.J. Development of novobiocin analogues that manifest anti-proliferative activity against several cancer cell lines. *J. Org Chem.* **2008,** *73*, 2130–2127.
30. Armstrong, H.K.; Koay, Y.C.; Irani, S.; Das, R.; Nassar, Z.D.; Australian Prostate Cancer BioResource, Selth, L.A.; Centenera, M.M.; McAlpine, S.R.; Butler, L.M. A novel class of Hsp90 C-Terminal modulators have pre-clinical efficacy in prostate tumor cells without induction of a heat shock response. *Prostate* **2016**, 76, 1546–1559.
31. Moses, M.A.; Henry, E.C.; Ricke, W.A.; Gasiewicz, T.A. The heat shock protein 90 inhibitor, (-)-epigallocatechin gallate, has anticancer activity in a novel human prostate cancer progression model. *Cancer Prev. Res. (Phila).* **2015,** *8*, 249–257.
32. Le Bras, G.; Radanyi, C.; Peyrat, J.-F.; Brion, J.-D.; Alami, M.; Marsaud, V.; Stella, B.; Renoir, J.-M. New novobiocin analogues as antiproliferative agents in breast cancer cells and potential inhibitors of heat shock protein 90. *J. Med. Chem.* **2007,** *50*, 6189–6200.
33. Radanyi, C.; Le Bras, G.; Marsaud, V.; Peyrat, J.-F.; Messaoudi, S.; Catelli, M.G.; Brion, J.-D.; Alami, M.; Renoir, J.-M. Antiproliferative and apoptotic activities of tosylcyclonovobiocic acids as potent heat shock protein 90 inhibitors in human cancer cells. *Cancer Lett.* **2008**, 274, 88–94.
34. Radanyi, C.; Le Bras, G.; Bouclier, C.; Messaoudi, S.; Peyrat, J.-F.; Brion, J.-D.; Alami, M.; Renoir, J.-M. Tosylcyclonovobiocic acids promote cleavage of the hsp90-associated cochaperone p23. *Biochem. Bioph. Res. Commun.* **2009,** *379*, 514–518.
35. Audisio, D.; Methy-Gonnot, D.; Radanyi, C.; Renoir, J.-M.; Denis, S.; Sauvage, F.; Vergnaud-Gauduchon, J.; Brion, J.-D.; Messaoudi, S.; Alami, M. synthesis and antiproliferative activity of novobiocin analogues as potential Hsp90 inhibitors. *Eur. J. Med. Chem.* **2014**, *83*, 498–507.
36. Radanyi, C.; Le Bras, G.; Messaoudi, S.; Bouclier, C.; Peyrat, J.-F.; Brion, J.-D.; Marsaud, V.; Renoir, J.-M.; Alami, M. Synthesis and biological activity of simplified denoviose-coumarins related to novobiocin as potent inhibitors of heat-shock protein 90 (hsp90). *Bioorg. Med. Chem. Lett.* **2008**, *18*, 2495–2498.

37. Audisio, D.; Messaoudi, S.; Cegielkowski, L.; Peyrat, J.-F.; Brion, J.-D.; Methy-Gonnot, D.; Radanyi, C.; Renoir, J.-M.; Alami, M. Discovery and biological activity of 6brcaq as an inhibitor of the Hsp90 protein folding machinery. *ChemMedChem.* **2011**, *6*, 804–815.
38. Messaoudi, S.; Audisio, D.; Brion, J.-D.; Alami, M. Rapid access to 3-(*N*-substituted)-aminoquinolin-2(*1H*)-ones using palladium-catalyzed C–N bond coupling reaction. *Tetrahedron* **2007**, *63*, 10202–10210.
39. Sauvage, F.; Fattal, E.; Al-Shaer, W.; Denis, S.; Brotin, E.; Denoyelle, C.; Blanc-Fournier, C.; Toussaint, B.; Messaoudi, S.; Alami, M.; Barratt, G.; Vergnaud-Gauduchon, J. Antitumor activity of nanoliposomes encapsulating the novobiocin analog 6brcaq in a triple-negative breast cancer model in mice. *Cancer Lett.* **2018**, *432*, 103–111.
40. Sauvage, F.; Franzè, S.; Bruneau, A.; Alami, M.; Denis, S.; Nicolas, V.; Lesieur, S.; Legrand, F.-X.; Barratt, G.; Messaoudi, S.; Vergnaud-Gauduchon, J. Formulation and *in vitro* efficacy of liposomes containing the Hsp90 inhibitor 6BrCaQ in prostate cancer cells. *Int. J. Pharm*. **2016**, 499, 101–109.
41. Mathieu, C.; Chamayou, Q.; Luong, T.T.H.; Naud, D.; Mahuteau, F.; Alami, M.; Fattal, E.; Messaoudi, S.; Vergnaud-Gauduchon, J. Synthesis and antiproliferative activity of 6BrCaQ-TPP conjugates for targeting the mitochondrial heat shock protein TRAP1, *Eur. J. Med. Chem.* **2022**, 229, 114052–114065.
42. Zhao, H.; Yan, B.; Peterson, L.B.; Blagg, B.S.J. 3-Arylcoumarin derivatives manifest anti-proliferative activity through hsp90 inhibition. *ACS Med. Chem. Lett.* **2012**, *3*, 327–331.
43. Bruneau, A.; Brion, J.-B.; Messaoudi, S.; Alami, M. A General Pd/Cu-catalyzed C-H heteroarylation of 3-bromoquinolin-2(*1H*)-ones. *Org. Biomol. Chem*. **2014**. 12, 8533–8541.
44. Wang, L.; He, W.; Yu, Z. Transition-metal mediated carbon–sulfur bond activation and transformations. *Chem. Soc. Rev.* **2013**, *42*, 599–621.
45. Pan, F.; Shi, Z.-J. Recent advances in transition-metal-catalyzed C–S activation: From thioester to (hetero)aryl thioether. *ACS Catal.* **2014,** *4*, 280–288.
46. Prokopcová, H.; Kappe, C.O. The Liebeskind–Srogl C-C cross-coupling reaction. *Angew. Chem. Int. Ed.* **2009**, *48*, 2276–2286.
47. Vabre, R. Fonctionnalisation directe de liaisons C-H et couplages croisés pour la formation de liaisons C-C et C-N: synthèse de purines 6,8,9-trisubstituées. PhD Thesis, Université Paris Sud - Paris XI, 2013.
48. Vabre, R.; Chevot, F.; Legraverend, M.; Piguel, S. Microwave-assisted Pd/Cu-catalyzed C-8 direct alkenylation of purines and related azoles: An alternative access to 6, 8, 9-trisubstituted purines. *J. Org. Chem.* **2011**, *76*, 9542–9547.
49. Benner, S.A. Understanding nucleic acids using synthetic chemistry. *Acc. Chem. Res.* **2004**, *37*, 784–797.
50. Jordheim, L.P.; Durantel, D.; Zoulim, F.; Dumontet, C. Advances in the development of nucleoside and nucleotide analogues for cancer and viral diseases. *Nat. Rev. Drug Discov.* **2013,** *12*, 447–464.
51. Sugahara, T.; Murakami, K.; Yorimitsu, H.; Osuka, A. Palladium-catalyzed amination of aryl sulfides with anilines. *Angew. Chem. Int. Ed.* **2014,** 53, 9329–9333.
52. Pellegatti, L.; Vedrenne, E.; Leger, J.-M.; Jarry, C.; Routier, S. First efficient palladium-catalyzed aminations of pyrimidines, 1, 2, 4-triazines and tetrazines by original methyl sulfur release. *Synlett* **2009**, 2137–2142.
53. Bruneau, L.A.; Roche, M.; Alami, M.; Messaoudi, S. 2-Aminobiphenyl Palladacycles: The "Most Powerful" Precatalysts in C–C and C–Heteroatom Cross-Couplings. *ACS Catal.* **2015**, *5*, 1386–1396.
54. Liu, J.; Robins, M.J. Fluoro, alkylsulfanyl, and alkylsulfonyl leaving groups in Suzuki cross-coupling reactions of purine 2'-deoxynucleosides and nucleosides. *Org. Lett.* **2005**, *7*, 1149–1151.

Sample Availability: Samples of the compounds are available from the authors.